



Inhibition of human leukocyte elastase, plasmin and matrix metalloproteinases by oleic acid and oleoyl-galardin derivative(s)

Gautier Moroy^a, Erika Bourguet^b, Martine Decarme^c, Janos Sapi^b, Alain J.P. Alix^{d,*}, William Hornebeck^c, Sandrine Lorimier^{c,e}

^a Université Paris Diderot, Molécules thérapeutiques in silico, INSERM UMR-S-973, Bât. Lamarck, 35 rue Hélène Brion, 75205 Paris Cedex 13, France

^b Université de Reims Champagne-Ardenne, CNRS UMR 6229, Institut de Chimie Moléculaire de Reims, Faculté de Pharmacie, IFR53 Biomolécules, 51 rue de Cognacq-Jay, 51096 Reims Cedex, France

^c Université de Reims Champagne-Ardenne, CNRS UMR 6237, Laboratoire de Biochimie Médicale, Faculté de Médecine, IFR53 Biomolécules, 51 rue de Cognacq-Jay, 51096 Reims Cedex, France

^d Université de Reims Champagne-Ardenne, Laboratoire de Spectroscopies et Structures Biomoléculaires, (EA4303), Faculté des Sciences, IFR53 Biomolécules, BP 1039, 51687 Reims Cedex2, France

^e Université de Reims Champagne-Ardenne, INSERM UMR-S926, Interface Biomatériaux/Tissus Hôtes, Faculté d'Odontologie, IFR53 Biomolécules, 51 rue Cognacq Jay, 51096 Reims Cedex, France

ARTICLE INFO

Article history:

Received 6 September 2010

Accepted 1 December 2010

Available online 10 December 2010

Keywords:

Leukocyte elastase

Plasmin

Matrix metalloproteinase

Oleic acid

Oleoyl-galardin

Molecular docking

ABSTRACT

Molecular modeling was undertaken at aims to analyze the interactions between oleic acid and human leukocyte elastase (HLE), plasmin and matrix metalloproteinase-2 (MMP-2), involved in the inhibitory capacity of fatty acid towards those proteases. The carboxylic acid group of the fatty acid was found to form a salt bridge with Arg²¹⁷ of HLE while unsaturation interacted with Phe¹⁹² and Val²¹⁶ at the S₃ subsite, and alkyl end group occupied S₁ subsite. In keeping with the main contribution of kringle 5 domain in plasmin–oleic acid interaction [Huet E et al. *Biochem Pharmacol* 2004;67(4):643–54], docking computations revealed that the long alkyl chain of fatty acid inserted within a hydrophobic groove of this domain with the carboxylate forming a salt bridge with Arg⁵¹². Finally, blind docking revealed that oleic acid could occupy both S'₁ subsite and Fn(II)₃ domain of MMP-2. Several residues involved in Fn(II)₃/oleic acid interaction were similarly implicated in binding of this domain to collagen.

Oleic acid was covalently linked to galardin (at P'₂ position): OL-GAL (CONHOH) or to its carboxylic acid counterpart: OL-GAL (COOH), with the idea to obtain potent MMP inhibitors able to also interfere with elastase and plasmin activity. OL-GALs were found less potent MMP inhibitors as compared to galardin and no selectivity for MMP-2 or MMP-9 could be demonstrated. Docking computations indicated that contrary to oleic acid, OL-GAL binds only to MMP-2 active site and surprisingly, hydroxamic acid was unable to chelate Zn, but instead forms a salt bridge with the N-terminal Tyr¹¹⁰. Interestingly, oleic acid and particularly OL-GALs proved to potently inhibit MMP-13. OL-GAL was found as potent as galardin (K_i equal to 1.8 nM for OL-GAL and 1.45 nM for GAL) and selectivity for that MMP was attained (2–3 log orders of difference in inhibitory potency as compared to other MMPs).

Molecular modeling studies indicated that oleic acid could be accommodated within S'₁ pocket of MMP-13 with carboxylic acid chelating Zn ion. OL-GAL also occupied such pocket but hydroxamic acid did not interact with Zn but instead was located at 2.8 Å from Tyr¹⁷⁶.

Since these derivatives retained, as their oleic acid original counterpart, the capacity to inhibit the amidolytic activity of HLE and plasmin as well as to decrease HLE- and plasmin-mediated pro MMP-3 activation, they might be of therapeutic value to control proteolytic cascades in chronic inflammatory disorders.

© 2010 Elsevier Inc. All rights reserved.

Abbreviations: HLE, human leukocyte elastase; Fn, fibronectin domain; MMP, matrix metalloproteinase; OL-GAL, oleoyl-galardin derivatives.

* Corresponding author: Université de Reims Champagne-Ardenne, IFR53 Biomolécules, Laboratoire de Spectroscopies et Structures Biomoléculaires (LSSBM, EA 4303), Faculté des Sciences, BP 1039, 51687 Reims Cedex2, France. Tel.: +33 6 73 87 93 43; fax: +33 3 26 08 56 61.

E-mail addresses: gautier.moroy@univ-paris-diderot.fr (G. Moroy), erika.bourguet@univ-reims.fr (E. Bourguet), martine.decarme@univ-reims.fr (M. Decarme), janos.sapi@univ-reims.fr (J. Sapi), alain.alix@univ-reims.fr (Alain J.P. Alix), william.hornebeck@univ-reims.fr (W. Hornebeck), sandrine.lorimier@univ-reims.fr (S. Lorimier).

1. Introduction

Unrestrained proteolytic activity constitutes the hallmark of non-healing wounds leading to the persistent inflammatory response at the wound site [1,2]. Proteases involved belong mainly to the serine- and metallo-peptidase families and originate from a variety of different cell types. Invading leukocytes and macrophages are considered as the main source of numerous proteases but keratinocytes at the wound edge, together with fibroblasts and endothelial cells, also participate in proteolysis [1–4]. Elevated levels of serine proteases as leukocyte elastase, plasminogen activators and plasmin together with a pleiade of metalloproteinases (MMPs) including collagenases, i.e. MMP-1, MMP-8, MMP-13, gelatinases, i.e. MMP-2, MMP-9, and stromelysins, i.e. MMP-3, MMP-10 and MMP-11, can be identified in non-healing chronic ulcers [5,6]. Serine proteases are the major inducers of pro MMP activation and besides can inactivate TIMP through proteolytic cleavage; Alpha-1 antitrypsin or alpha-2 antiplasmin, in turn, are targets of MMPs, thus creating a local environment with large excess of proteolytic activity directed against growth factors or matrix constituents [7–9]. The use of substances that can disrupt this degradation cascade might therefore be considered as an effective therapy towards healing of a chronic wound. Long chain unsaturated fatty acids, as oleic acid, have been reported to interfere with the activity of several enzyme systems as inhibiting prolyl endopeptidase [10], chymase [11], proteasome [12] or tissue factor–factor VIIa complex activities [13]. Our previous investigations and data from the literature, indicated that oleic acid could similarly inhibit leukocyte elastase and gelatinase activities towards synthetic substrates and elastin [14–17]. It can also impede plasmin-mediated prostromelysin-1 activation [18]. We have first confirmed these findings and identified by molecular modeling studies, the enzyme exosites involved in the binding of oleic acid to those proteases. Coupling of oleic acid to leukocyte elastase inhibitors as peptide, acyl saccharin or heparin(s) was found to improve the inhibitory capacity of inhibitors and to ameliorate their biodisponibility or to add novel functions [14,19,20]. By analogy, in keeping with the main contribution of MMPs in non-healing wounds, we derivatized galardin, a potent broad spectrum MMP inhibitor, with oleic acid and studied the properties of these derivatives (Fig. 1).

2. Experimental procedures

2.1. Reagents

Human plasmin (6-AHA, lysine free) was purchased from Calbiochem represented from VWR International and human leukocyte elastase came from Elastin Products Company (St. Louis, MO, USA). Human pro MMP-1, pro MMP-2, pro MMP-8, pro MMP-9, pro MMP-13, as well as catalytic forms of MMP-3, MMP-7 and MMP-14 were also from Calbiochem (VWR, Fontenay/Bois, France).

The synthetic chromogenic substrate S-2251 (H-D-Val-Leu-Lys *p*-nitroanilide) for plasmin determination and *N*-MeO-Suc-Ala-Ala-Pro-Val *p*-nitroanilide for elastase assay were obtained from Sigma (St-Quentin Fallavier; France) and Chromogenix (Instrumentation Laboratory, Paris, France), respectively. Fluorescent quenched substrates for MMP activity determination: Mca-Pro-Leu-Gly-Leu-Dap-Ala-Arg-NH₂ (MMP-2, MMP-8, MMP-13, MMP-14) and 6-(7-Nitro-benzo(2,1,3)oxadiazol-4-ylamino)-hexanoyl-Arg-Pro-Lys-Pro-Leu-Ala-Nva-Trp-Lys(7-dimethylaminocoumarin-4-yl)-NH₂ (MMP-3) were obtained from Bachem (Weil am Rhein, Germany); DNP-Pro-Cha-Gly-Cys(Me)-His-Ala-Lys(N-Me Abz)-NH₂ (MMP-1, MMP-9) and Mca-Pro-Leu-Gly-Leu-Dpa-Ala-Arg-NH₂ (MMP-7) were obtained from Calbiochem. *Cis*-9-octadecenoic acid (oleic acid, C18) was purchased from Sigma. *N*-Methylmorpholine (NMM), *tert*-butylcarbazate, tryptophan and hydroxylamine hydrochloride were purchased from Acros Organics (Noisy-Le-Grand, France).

2.2. Synthesis and characterization of oleoyl-galardin derivatives: OL-GAL (COOH) (compound 6) and OL-GAL (CONHOH) (compound 7)

For the synthesis of oleoyl-galardin derivatives (6 and 7) we developed a linear pathway: successive 4-(4,6-dimethoxy-1,3,5-triazin-2-yl)-4-methyl-morpholinium chloride (DMTMM) [21] mediated couplings were carried out between oleic-acid hydrazide (1) and *L*-Boc-tryptophan 2 and thereafter between the obtained product (3) and a conveniently functionalized succinic ester acid (4) [22] (Schemes 1 and 2, Supporting Information). Carboxylic acid or hydroxamic acid-type zinc-binding groups were introduced by simple functional group transformation

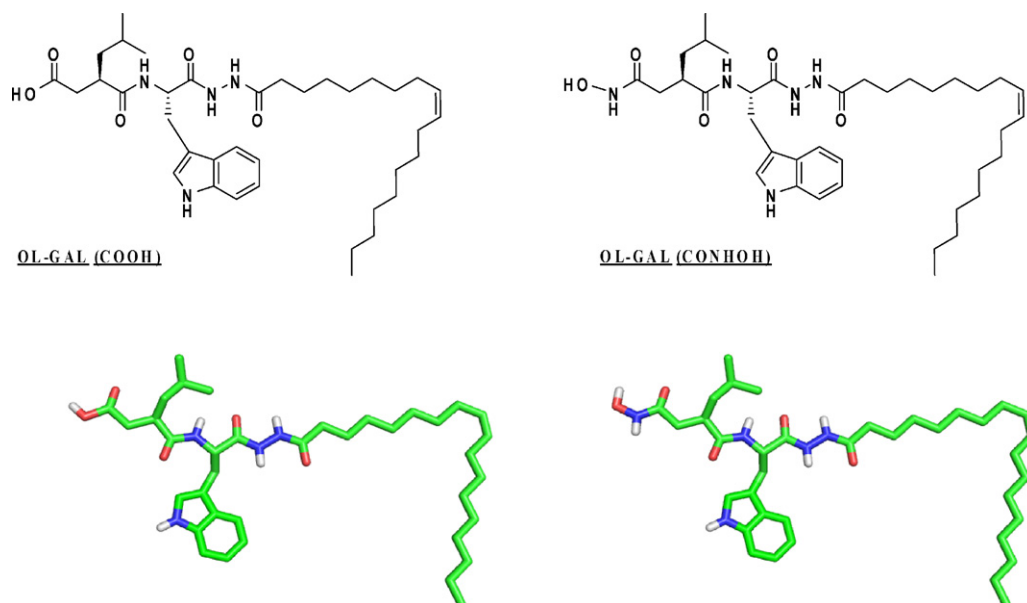
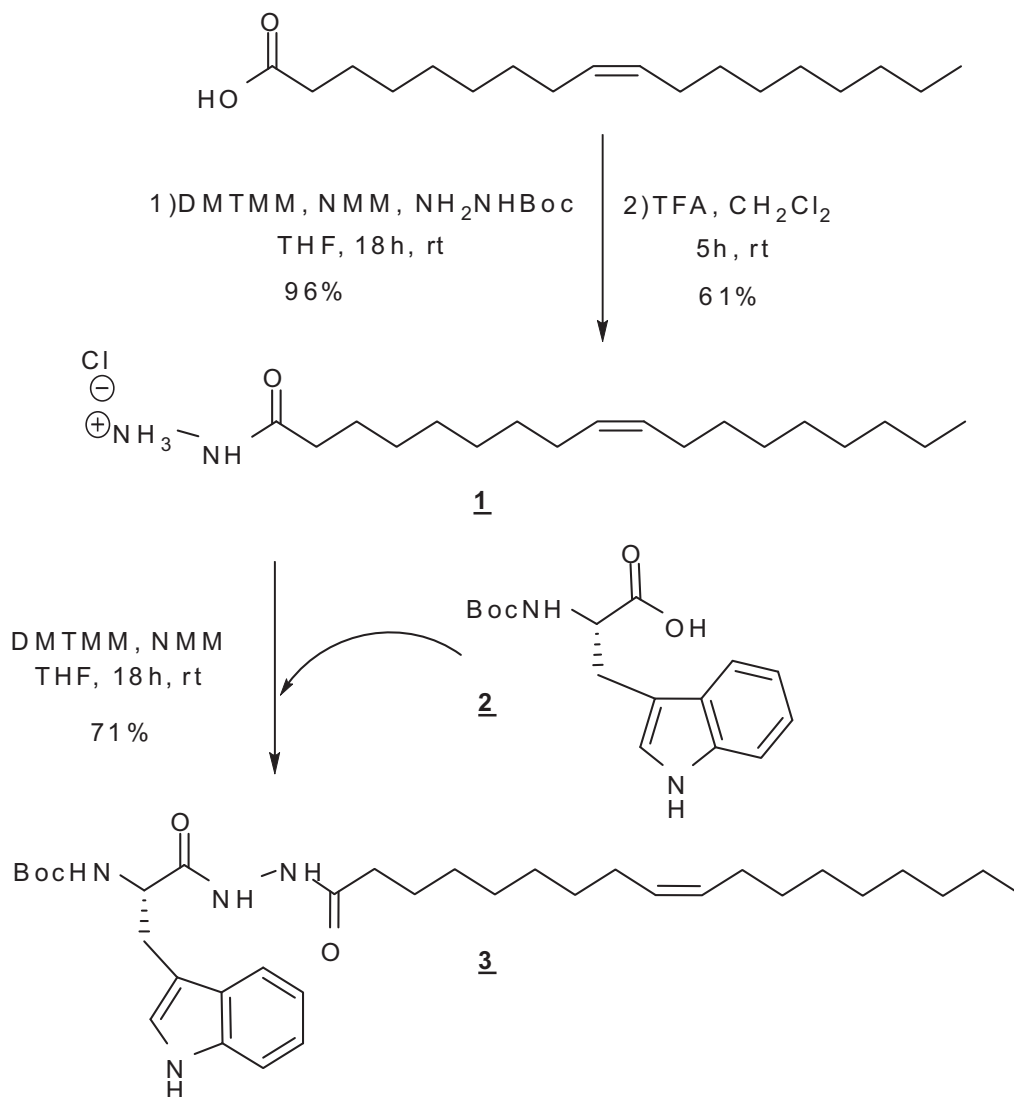


Fig. 1. Structures of oleoyl-galardins.



Scheme 1.

affording oleoyl-galardin derivatives **OL-GAL(COOH)** and **OL-GAL(CONHOH)**, respectively (Fig. 1).

Reactions and products were routinely monitored by thin-layer chromatography (TLC) on silica gel (KIESELGEL 60 PF254, Merck). Flash chromatography was performed on Kieselgel 60 (40–63 μm , Merck). Melting points were determined on a Reichert Thermovar hot-stage apparatus and are uncorrected. UV spectra were recorded in methanol solution on a Unicam 8700 UV/vis apparatus. IR spectra were measured on a Perkin-Elmer Spectrum BX FTIR instrument. ^1H NMR (300 MHz) and ^{13}C NMR (75 MHz) spectra were recorded on a Bruker AC300 spectrometer using TMS as internal standard, chemical shifts were given in ppm (δ). Couplings expressed as s, br s, d, t, and m correspond to singlet, broad-singlet, doublet, triplet and multiplet, respectively. Mass spectra were recorded on a MSQ ThermoFinnigan apparatus using chemical ionization (CI) method. Optical rotations were measured on a Perkin-Elmer 241 polarimeter.

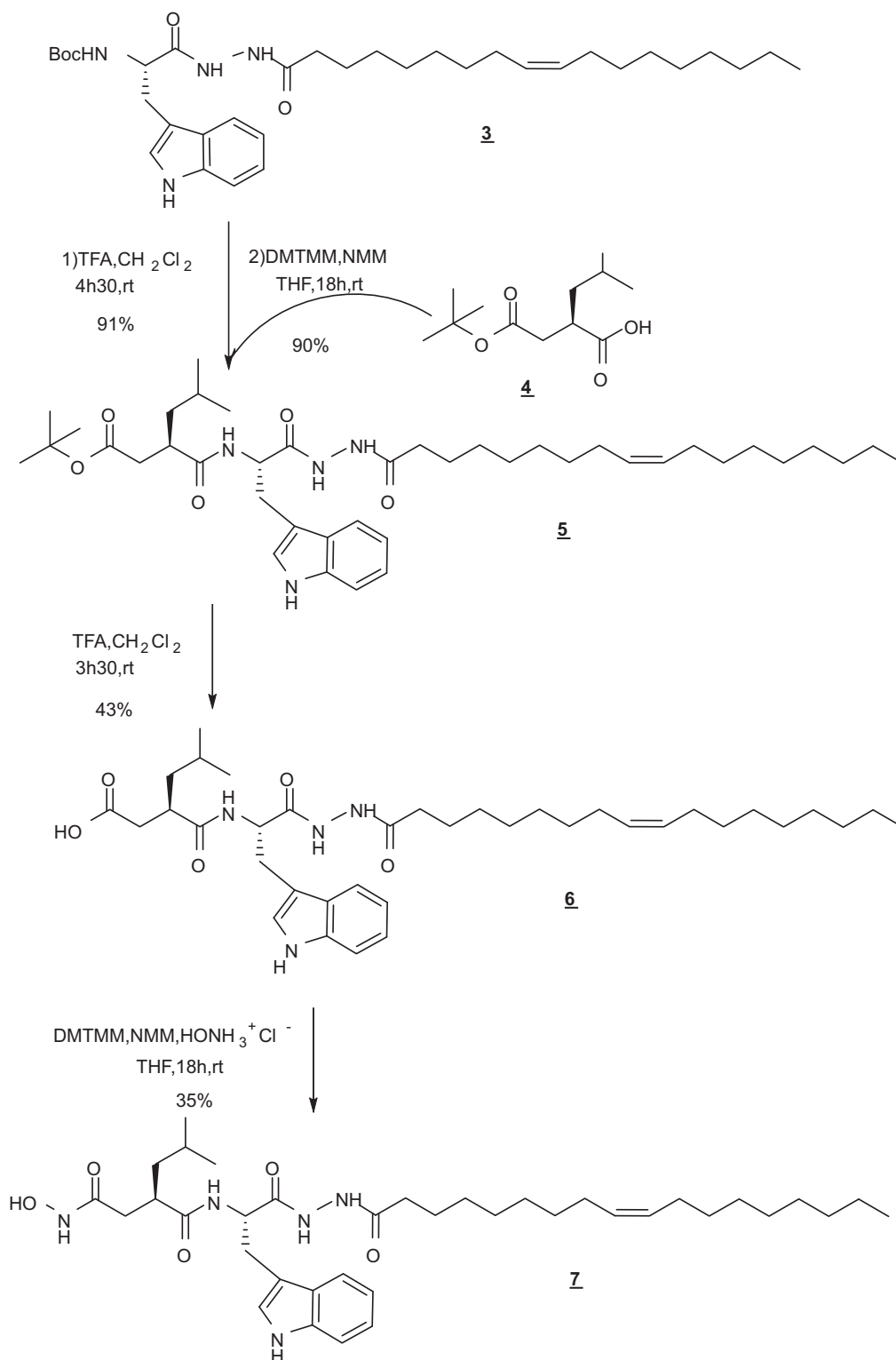
2.3. Enzyme assays

The amidolytic activity of HLE was assayed using *N*-MeO-Suc-Ala-Ala-Pro-Val-*p*-nitroanilide as a substrate [15,20]. The release of *p*-nitroaniline was monitored by recording the absorbance with

a λ_{max} , equal to 405 nm, and low-binding multiwell microplate reader (Immulan 1B from Dutscher) operating in the kinetic mode. Reaction was performed in 150 mM NaCl containing Tris buffer pH 8.0, with 300 ng of HLE, 1 mM substrate and increasing concentration of oleic acid and galardin derivatives from 1 mM to 1 μM . Kinetic data were collected for 30 min, a period where reaction rates remain linear. Activities in the presence of inhibitor (v_i) were normalized to controls determined in the absence of inhibitor (v_o).

Plasmin amidolytic activity was monitored using the chromogenic substrate S-2251 as described [18]. Briefly, 200 μL of 10 mM Tris HCl buffer, pH 8.1, containing 12 nM plasmin and 0.3 mM of substrate were added in 96-well low binding titration plate (Nunc) and incubated in the presence or absence of oleic acid and oleoyl-galardins (0–10 μM) at room temperature. Release of *p*-nitroaniline was followed continuously for 30 min; during such time of incubation, reaction rates were linear. Plasmin unit is defined as the amount of enzyme that will hydrolyse 1 μmol of H-D-Val-Leu-Lys *p*-nitroanilide.

Full length pro MMP (10–20 nM) were first activated by incubating the proenzymes in 150 mM NaCl, 5 mM CaCl_2 , 50 mM Tris HCl, pH 7.5, with 1 mM *p*-aminophenyl mercuric acetate (APMA) for 1 h (pro MMP-1, -2, -9, -13) or 3 h (pro MMP-8) at 37 $^\circ\text{C}$.



Scheme 2.

Full activation for each enzyme was assessed by Western Blot. Each enzyme was further active site-titrated using a standard preparation of TIMP1 to allow accurate determination of E_0 .

The inhibitory effect of oleic acid and oleoyl-galardin derivatives against MMPs were analyzed using 5–50 ng active enzyme and 1–10 μ M fluorescent quenched substrates. Five to 50 ng of MMPs species were preincubated for 15 min at 22 °C with 0–50 μ M fatty

acid and derivatives in 50 mM Tris test buffer, pH 7.5, containing 150 mM NaCl and 5 mM CaCl₂. The assays were initiated by adding 1 μ M (MMP-3), 2 μ M (MMP-2, MMP-7, MMP-8, MMP-13, MMP-14), 10 μ M (MMP-1, MMP-9) corresponding substrates. The final concentration of dimethyl sulfoxide (Me₂SO) to dissolve oleic acid(s) and fluorogenic substrate never exceeded 1% (v/v). The reaction was allowed to proceed for 20 min at 22 °C with the exception of MMP-3 for which activity was followed at 37 °C.

The rate of substrate cleavage was determined in quadruplicate for oleic acid or derivatives concentrations examined, using a Perkin Elmer LS 50B spectrofluorimeter with excitation and emission wavelengths of 326 and 465 nm respectively for MMP-2, -7, -8, -13, -14, and 360 and 465 nm respectively for MMP-1, -9 and catalytic MMP-3. Less than 5% of the substrate was hydrolyzed during the rate measurements and kinetics were linear in the presence or absence of inhibitor. Non-linear regression analysis with the Graft computer software (Leather-barrow RJ, Erithacus Software) allowed us to calculate the best estimates of the equilibrium dissociation constant of the enzyme-inhibitor complex or the inhibition constant K_i , using the integrated equations:

$$\frac{v_i}{v_o} = 1 - \frac{([E]_o + [I]_o + K_i) - \{([E]_o + [I]_o + K_i)^2 - 4[E]_o[I]_o\}^{1/2}}{2[E]_o}$$

where v_i is the rate of substrate hydrolysis in the presence of inhibitor, v_o is the rate in its absence; $[E]_o$ and $[I]_o$ are the initial concentrations of enzyme and oleic acid derivatives, respectively [17].

All inhibition curves are fitted from means of three separate experiments (the standard deviation never exceeding 10% of the mean).

2.4. Analysis of pro MMP activation by Western Blot

Human plasmin (65 nM) or human leukocyte elastase (300 ng) was preincubated in the presence of oleoyl-galardin derivatives (0.1–10 μ M) in 50 mM Tris HCl buffer pH 7.8, containing 150 mM NaCl and 5 mM CaCl_2 for 15 min at 37 °C. Pro MMP-3 (40 ng) (Biogenesis, Abcys, Paris, France) was then added and the reaction was allowed to proceed for 4 h at 37 °C. At the end of the incubation, aprotinin (1 mg/mL) was added to inactivate serine peptidases.

MMP-3 was analyzed by Western Blot. Samples were submitted to sodium dodecyl sulphate-polyacrylamide gel electrophoresis (SDS-PAGE) in 10% (w/v) acrylamide under non-reducing conditions and proteins were electroblotted to PVDF membranes (Immobilon-P from Millipore, VWR, Fontenay/Bois, France). The membranes were blocked with 5% (w/v) non-fat dry milk (Biorad, Ivry/Seine, France) in 50 mM TBS buffer, pH 7.5, containing 150 mM NaCl for 2 h at 20 °C. The blotted proteins were probed with primary antibody diluted in TBS-Tween (0.1%, v/v) (TBS-T) containing 1% non-fat dry milk (w/v) (Biorad) for a night at 4 °C. Monoclonal antibody against human MMP-3 (Ab-1, IM36, Calbiochem, VWR) was used at 1/1000. After extensive washings with TBS-T, the membranes were incubated with peroxidase-conjugated goat anti-mouse IgG (Immunotech, Marseille, France) (1/10 000) for 1 h at 20 °C. After extensive washings with TBS-T, the immunoreactive proteins were revealed by staining with enhanced chemiluminescent detection reagents or with NBT/BCPI reagent (GE Healthcare, VWR).

2.5. Molecular modeling

AutoDock 4.0 program [23,24] was used to perform the computational molecular docking. The molecular docking computations attempt to predict the structure of a complex formed between a small flexible molecule (ligand) and its target says a protein. Numerous positions and conformations of the ligand at the surface of the protein are generated using a stochastic search method (here we used the hybrid global local search Lamarckian Genetic evolutionary Algorithm) and the resulting binding modes are evaluated by the docking program through the choice of a scoring function. In the case of AutoDock 4, the used scoring function takes into account the following terms of energy: van der Waals, electrostatic, hydrogen bond, desolvation and torsional.

AutoDockTools (ADT) package was employed to prepare the input files necessary to the docking procedures and to analyze the

docking results. The figures have been drawn using PyMol program (DeLano WL 2002 The. PyMol Molecular Graphics System, Palo Alto, CA. <http://www.pymol.org>).

2.5.1. Ligand and protein preparation

Oleic acid, oleoyl-galardin OL-GAL (CONHOH) and its carboxylic acid analog OL-GAL (COOH) were built using the module BIOPOLYMER of Insight98 software package (MSI, Inc., San Diego, CA, USA). The partial charges of these compounds were calculated with the Gaussian 03 program [25] using a 6-31G* basis set. The 3D structures of the HLE [26], the full-length human MMP-2 [27], the kringle 5 domain from the human plasmin [28] and the human MMP-13 [29] were retrieved from the Brookhaven Protein Data Bank, their PDB codes being respectively 1PPF, 1CK7, 2KNF and 1YOU. While all the inhibitor atoms, water molecules and ions were removed from the crystal structures, the Zn atom was kept in the catalytic site of the MMPs. Experimentally, the MMP-2 is active when the propeptide is released. The presence of this domain obstructs the catalytic site of the MMP-2 and prohibits experimentally its proteolytic activity. Therefore, we have also removed the residues corresponding to this domain, i.e. residues 31–109 (the signal peptide was not solved). Protonation states of all ionizable residues were computed using PROPKA program [30,31]. Gasteiger charges were calculated for the atoms from the HLE, MMP-2, plasmin kringle 5 domain and MMP-13 by ADT package.

2.5.2. Docking protocol

From affinity grids for each type of atom constituting the oleic acid, an electrostatic and a desolvation map were calculated. Since we cannot *a priori* define where oleic acid is able to bind at the surface of the HLE and the MMP-2, two grid sizes were defined: the first one on the whole protein to perform “blind docking” and the second one focusing on the best affinity sites highlighted by the docking results with the first grid. In the case of MMP-13 and kringle 5 plasmin, one grid was calculated and centered respectively on MMP catalytic site or on plasmin binding site.

The size of the first grid for HLE was 126 Å × 126 Å × 126 Å with a 0.44 Å spacing; the second one was 126 Å × 126 Å × 126 Å with 0.30 Å spacing. For the MMP-2, the first grid was only positioned on the fibronectin domains and the catalytic domain; due to the large size of this protein, the hemopexin domain, which has no oleic acid binding activity, was not taken into account. The dimension of the first and the second grid were respectively 96 Å × 126 Å × 120 Å with a 0.64 Å spacing and 126 Å × 126 Å × 126 Å with a 0.30 Å spacing. The latter grid was employed for the MMP-13 and the kringle 5 of plasmin.

We employed the Lamarckian genetic algorithm (LGA) for ligand conformational searching. Four independent runs of docking computations were done with, for each, the following parameters: 250 LGA operations, a population size of 250 individuals, a maximum of 2 000 000 energy evaluations and a maximum of 2700 generations. The default parameters for the LGA operation and Sollis and Wet local search were used.

During the docking computations, the maximum of torsions angles were allowed to be rotatable. For the oleic acid, the torsion angle corresponding to the double bond between C9 and C10 was the only one which was kept rigid. In the oleoyl-galardin compounds, the ω dihedral angles of the peptidic bonds were frozen to 180°.

3. Results

3.1. Analysis of the binding mode of oleic acid to leukocyte elastase and plasmin by molecular modeling

A series of investigations evidenced that oleic acid could inhibit leukocyte elastase either in a non-competitive, competitive or

mixed modes with K_i in the 3–17 μM range [14,15]. Positively charged Arg [32] and Phe–Ala residues [15], located at the vicinity of the enzyme active site have been suggested to participate in fatty acid binding to enzyme since amide derivative of the oleic acid and saturated counterpart as stearic acid lacked inhibitory activity.

Blind docking of oleic acid at the surface of HLE highlights only one region of interest localized within enzyme active site.

Accordingly, HLE catalytic site was further embedded in a second affinity grid to perform more precise computations.

For the molecular docking analysis, we focus on the docked conformations which are the more credible interaction structures. Based on AutoDock 4 scoring function that computes the binding energy of each docked conformation, the most confident binding modes are then those with the lowest energy models.

As in the first grid, the lowest energy models are seen to be in a similar position and orientation. Fig. 2a indicates that oleic acid can extend from S_1 to S_5 HLE subsites. Interaction is then characterized by numerous van der Waals contacts involving His⁵⁷, Leu⁹⁹, Arg¹⁷⁷, Cys¹⁹¹, Phe¹⁹² \rightarrow Ser¹⁹⁵ and Ala²¹³ \rightarrow Arg²¹⁷. Moreover, oleic acid forms a salt bridge between its carboxylic group and the guanidinium group of the Arg²¹⁷ which lies within 10–15 Å of Ser¹⁹⁵ at the catalytic center of HLE. Besides, the unsaturated bond interacts with Phe¹⁹² and Val²¹⁶ at the S_3 subsite while alkyl end group is inserted in the S_1 subsite.

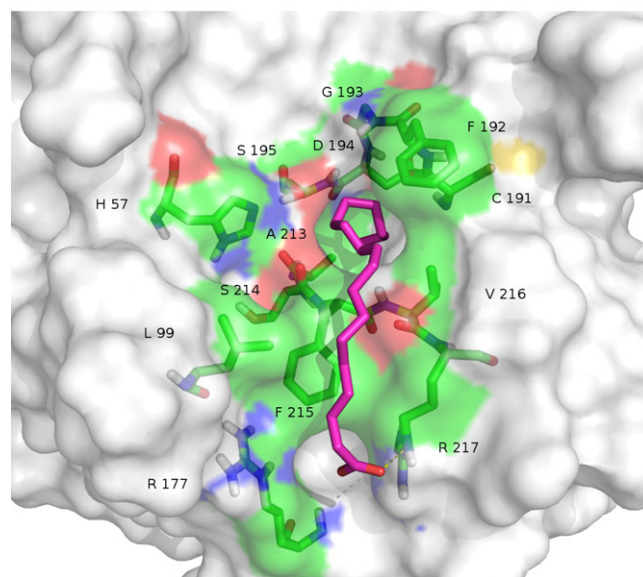
Oleic acid inhibition of plasmin-mediated pro MMP-3 activation was previously reported to be reproduced using miniplasmin but not microplasmin; also surface plasmon resonance analysis revealed that the fatty acid exhibited a higher affinity for K_5 as compared to other kringle domains of human plasmin [18].

Plasmin overall structure is not yet solved but those of individual domains are available and docking computations of oleic acid have been carried out on the kringle 5 domain. The lowest energy model of the interaction of fatty acid with this domain is characterized by the insertion of the long alkyl chain in a groove formed by: His⁵¹³, Ile⁵¹⁵, Phe⁵¹⁶, Asp⁵³⁵, Asp⁵³⁷, Trp⁵⁴², Tyr⁵⁴⁴, Leu⁵⁵¹, Tyr⁵⁵² and Tyr⁵⁵⁴ and the presence of a salt bridge between the carboxyl group of oleic acid and Arg⁵¹² (Fig. 2b).

3.2. Interaction between oleic acid and matrix metalloproteinases

We previously evidenced that oleic acid inhibited MMP-1 and MMP-2 with K_i equal to 59.6 μM and 4.3 μM , respectively [17]. The highest inhibitory capacity of this unsaturated fatty acid towards MMP-2 versus MMP-1 was here confirmed (Fig. 3A). No or only weak inhibition of MMP-3, MMP-8 and MMP-14 was observed but oleic acid proved to potentially interfere with MMP-13 activity: $K_i = 0.4 \mu\text{M}$ (Fig. 3A, Table 1). We therefore undertook molecular modeling studies at aim to define the interaction of oleic acid with MMP-2 and MMP-13, respectively (Fig. 3B). The lowest energy models of the oleic acid interacting with MMP-2 as first obtained by blind docking, are essentially localized at two sites on MMP-2 surface. The first one was identified as the S_1 enzyme pocket filled with fatty acid chain while the carboxylic acid group was exposed to the solvent. Such occupancy was in keeping with our previous data showing that such subsite could accommodate long alkyl side chains [33,34]. The second site of interaction was identified as the 3rd fibronectin type II (Fn II) domain. Thus, docking computations restricted to the 3rd Fn-II domain were performed using a second grid to precisely characterize oleic acid interactions. Fig. 3Ba shows that the unsaturated bond forms van der Waals interaction with Phe³⁵⁵, Trp³⁷⁴, Tyr³⁸¹ and Trp³⁸⁷ while the carboxylic acid group interacts via an H-bond with the phenolic group from Tyr³⁸¹, via a salt bridge with the guanidinium group of the Arg³⁸⁵ and via van der Waals type binding interactions with Leu³⁵⁶.

a HLE



b plasmin

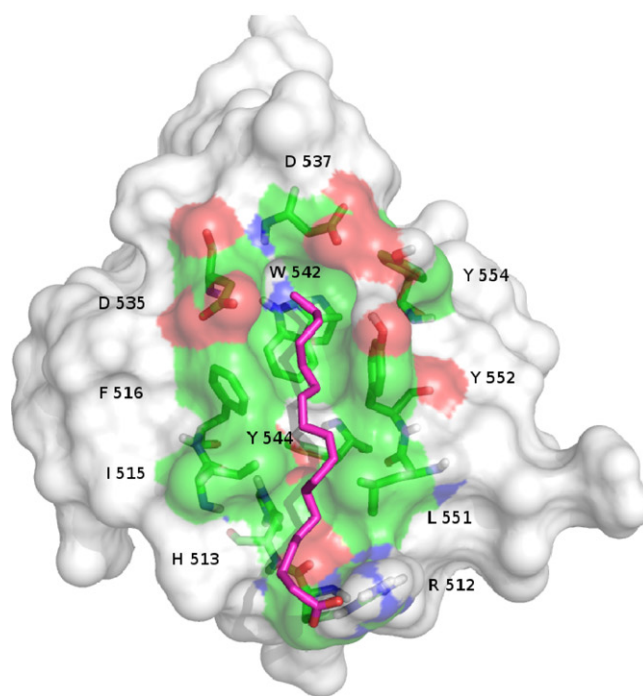
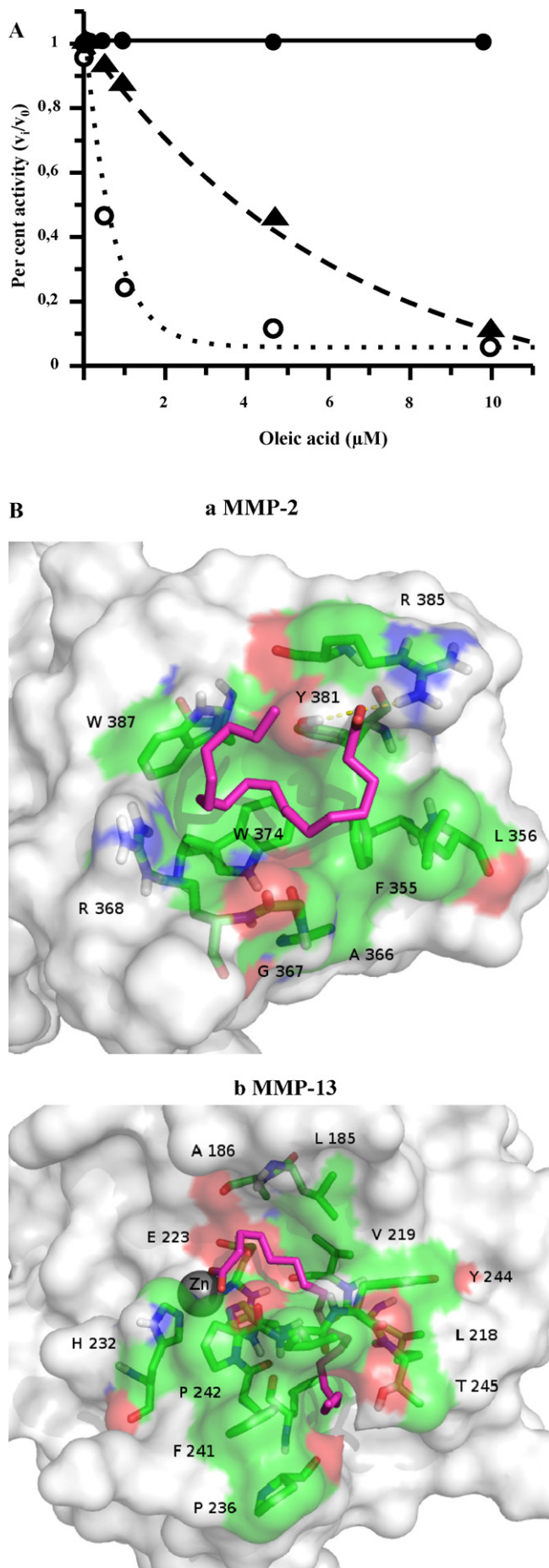


Fig. 2. Molecular docking of the interaction between oleic acid and a) HLE, b) human kringle 5 plasmin domain. All the non-polar H atoms have been removed for a better visualization. While the accessible surface area of the protein is displayed, the oleic acid and the residues implicated in the interaction are in stick representation. The C atoms from these latter and from oleic acid are colored in green and in magenta, respectively.

The lowest energy models obtained for the interaction between oleic acid and MMP-13 is localized in the catalytic site. The long alkyl chain lies within the S_1 subsite (Leu²¹⁸, Val²¹⁹, His²²², Gly²³⁷, Leu²³⁹ and Phe²⁴¹ \rightarrow Thr²⁴⁵) while the carboxylic acid function chelates the Zn ion (Fig. 3Bb).

3.3. Inhibition of MMPs by oleoyl-galardin derivatives

Derivatization of the carboxylic acid group of oleic acid to an hydroxamic acid was found previously to improve by 2–3 log



orders the inhibitory capacity of the compound towards MMP-2 [35]. To that line we incorporated such fatty acyl side chain to the P₂ site of galardin, a potent broad spectrum inhibitor of MMPs (Table 1) [36]. The carboxylic acid analogue of OL-GAL (CONHOH), as designated OL-GAL (COOH) was synthesized. The inhibitory potency of these compounds, as compared to parent molecules, i.e. oleic acid and galardin, towards eight MMPs is reported on Table 1. With the exception of MMP-13, both compounds exhibited higher K_i values as compare to galardin. Also, apart MMP-7, hydroxamic acid derivative appeared more potent than carboxylic acid counterpart, first suggesting that the galardin moiety was driving the inhibition at least for gelatinases and MMP-1. Importantly, OL-GALs can be considered as potent (K_i in the 1.8–5.1 nM range) and selective for MMP-13 (2–3 log difference in K_is between MMP-13 and other MMPs).

Using the first grid, the biggest which encompasses both MMP-2 active site and Fn(II) domains, docking computations indicated that, contrary to oleic acid, OL-GAL (CONHOH) binds to MMP-2 active site. The second grid was then centered to active site; the lowest energy model of OL-GAL (CONHOH) indicated that this compound was unable to chelate Zn in the active site. Instead, the hydroxamic acid group forms a salt bridge with N-terminal end of Tyr¹¹⁰, while the long alkyl chain was inserted into the S₁ pocket. Indole ring, in turn, now occupies the S₁ subsite where it interacts via an H-bond with the carbonyl group of the Ala¹⁹⁴ peptidic bond (Fig. 4a).

Oleoyl-galardin (OL-GAL (CONHOH)) binds to MMP-13 in a similar binding mode as to MMP-2 with no chelation of Zn ion of enzymes, penetration of long alkyl chain into the S₁ pocket and insertion of indole ring in the S₁ subsite (Fig. 4b). Besides, another strong interaction was highlighted where hydroxamic acid group was found close (2.8 Å) to the oxygen atom of the phenolic group of Tyr¹⁷⁶. Enzyme flexibility could allow a rotation of the bond between the O-atom and the aromatic C of the phenolic group to form a canonical H-bond, likely present in the natural binding mode between partners.

3.4. Influence of OL-GAL (CONHOH) on the leukocyte elastase and plasmin-mediated pro MMP-3 activation

We first analyzed the inhibitory capacity of OL-GAL (CONHOH) and OL-GAL (COOH) towards HLE amidolytic activity. Fig. 5 shows that the carboxylic acid-type derivative displayed high potency (IC₅₀ = 0.62 μM) against this enzyme but lower inhibition was observed with the hydroxamic acid counterpart (IC₅₀ = 8.75 μM). Docking computations indicated that the COOH end group of OL-GAL (COOH) but not its CONHOH counterpart can form a salt bridge with Arg²¹⁷ (not shown). Stromelysin-1 (MMP-3) displays a broad specificity towards extracellular matrix components and occupies a central position in proteolytic cascades leading to collagenolysis and elastolysis [37,38]. Pro MMP-3 can be activated by several serine proteases including HLE and plasmin. Incubation of 30 nM pro MMP-3 with 80 nM HLE for 15 min at 22 °C led to a total conversion of zymogen, i.e. 57 kDa to a 48 kDa and 28 kDa species. Such activation was inhibited by 50%, in average, following

Fig. 3. (A) Inhibition of collagenases 1 and 3 (MMP-1 ●-●, MMP-13 ○-○) and gelatinase A (MMP-2 ▲-▲) by oleic acid. abscissa: concentration of oleic acid (μM); ordinates: per cent activity (v_i/v₀); v_i: rate of substrate hydrolysis in presence of oleic acid; v₀: rate of substrate hydrolysis in absence of oleic acid. Inhibition curves are fitted from means of 3 separate experiments (the standard deviation never exceeding 10% of the mean).

(B) Molecular docking of the interaction between oleic acid and a) human MMP-2, b) human MMP-13. All the non-polar H atoms have been removed for a better visualization. While the accessible surface area of the protein is displayed, the oleic acid and the residues implicated in the interaction are in stick representation. The C atoms from these latter and from oleic acid are colored in green and in magenta, respectively. Zn in the catalytic site is represented as a grey sphere.

Table 1

Inhibition of MMPs by galardin, oleic acid and oleoyl-galardin derivatives towards MMPs (K_i s values, expressed in nM), HNE and Plasmin (IC₅₀ values expressed in nM). All data are means of four separate determinations—the standard deviations are indicated in brackets.

	MMP-1	MMP-2	MMP-3	MMP-7	MMP-8	MMP-9	MMP-13	MMP-14	HLE	Plasmin
Galardin [®]	0.8 (0.35)	4.3 (0.78)	28 (2.5)	16 (1.6)	1.2 (0.47)	0.74 (0.11)	1.45 (0.13)	5.7 (0.77)	NI ^a	NI
Oleic acid	NI	4300 (1995)	NI	6500 (1868)	NI	6400 (1824)	413 (99)	NI	3000–16 000 ^b	3500 (600)
OL-GAL (CONHOH)	281 (103)	147 (27)	54 (10)	670 (142)	1790 (125)	46 (6.7)	1.8 (0.74)	2290 (515)	8755 (900)	8346 (780)
OL-GAL (COOH)	NI	518 (75)	543 (138)	75 (9.7)	4114 (1187)	722 (411)	5.14 (1.6)	NI	622 (88)	751 (107)

^a NI: non-inhibitor.

^b See references [14,15].

preincubation of HLE with 10 μ M of either OL-GAL (CONHOH) or OL-GAL (COOH) prior to addition of pro MMP-3 (Fig. 5 inset).

Similarly, as found with HLE, upon addition of 65 nM plasmin, pro MMP-3 was activated to mature MMP-3 (Fig. 6). Preincubation of plasmin with increasing concentration of OL-GAL (CONHOH) from 0.1 to 10 μ M led to the inhibition of the conversion of

zymogen to enzyme active form. A nearly complete inhibition was attained at 10 μ M of this compound; for sake of comparison 50 μ M oleic acid inhibited plasmin-mediated pro MMP-3 activation by 59% [18] similarly as OL-GAL (COOH).

4. Discussion

Long chain unsaturated fatty acids, with C16 or more, were previously reported to inhibit the amidolytic and elastolytic activity of leukocyte elastase while leaving no inhibitory capacity towards pancreatic elastase, trypsin and α -chymotrypsin [14–16]. At oleic acid concentration leading to substantial loss of HLE activity, inhibition was competitive [15] and, consistent with earlier premises, we have evidenced by extensive molecular modeling study, that oleic acid could lie within the extended enzyme hydrophobic pocket. The carboxylic acid group of oleic acid forms a salt bridge with Arg²¹⁷ of enzyme, while Phe¹⁹² interacts with unsaturated bond and alkyl chain of fatty acid points towards S₁ subsite of elastase.

Binding to enzyme exosites, distant from active center, constitutes a novel approach in the control of proteolysis since it can improve the selectivity of inhibitor and impede the adsorption of protein to matrix macromolecules as elastin or

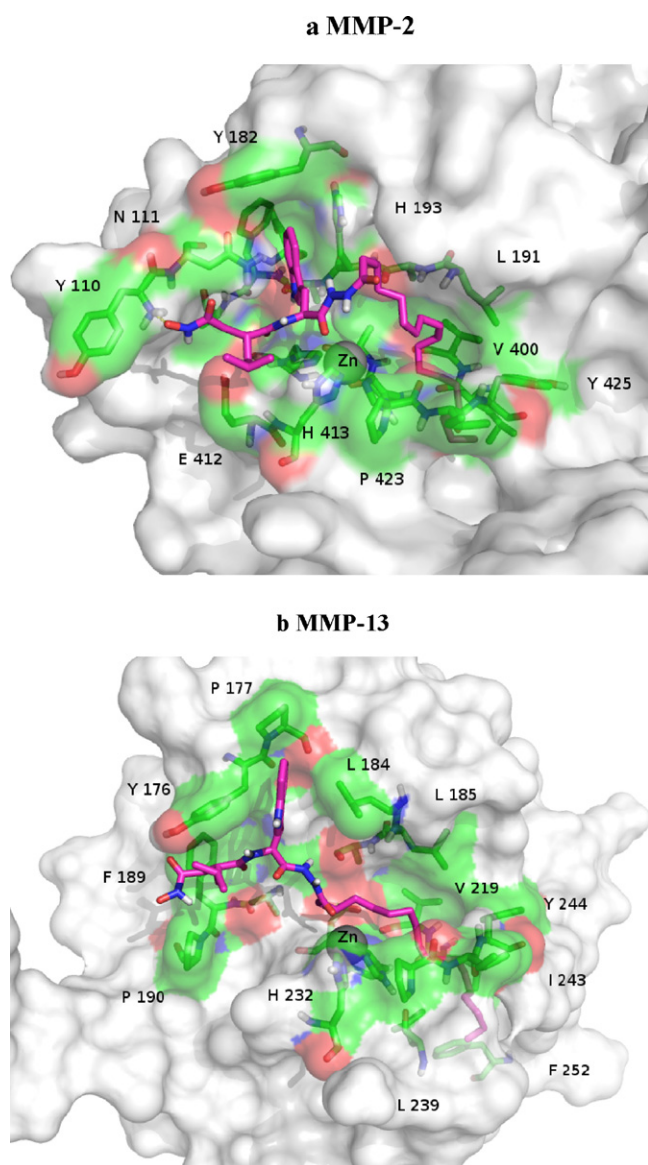


Fig. 4. Molecular docking of the interaction between oleoyl-galardin (CONHOH) and a) human MMP-2, b) human MMP-13. All the non-polar H atoms have been removed for a better visualization. While the accessible surface area of the protein is displayed, the oleic acid and the residues implicated in the interaction are in stick representation. The C atoms from these latter and from oleoyl-galardin (CONHOH) are colored in green and in magenta, respectively. Zn in the catalytic site is represented as a grey sphere.

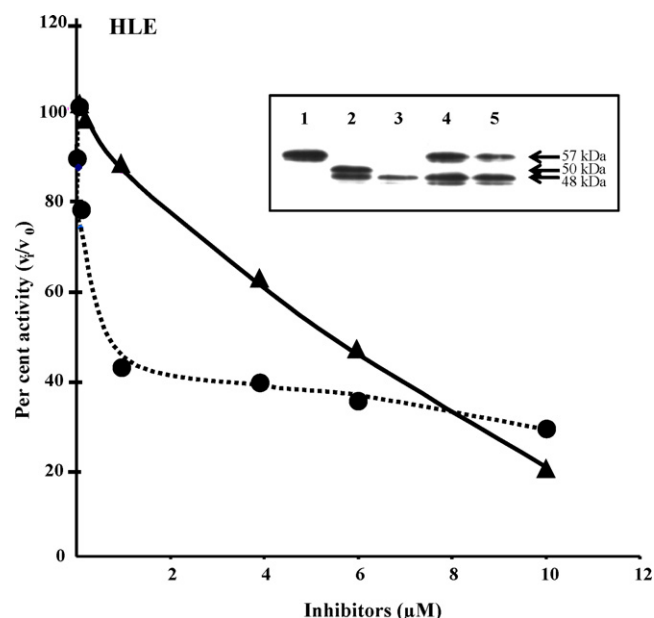


Fig. 5. Influence of oleoyl galardin derivatives on leukocyte elastase activity. abscissa: OL-GAL (CONHOH): \blacktriangle ; OL-GAL (COOH): \bullet ; concentration (μ M); ordinate: per cent activity (v_i/v_0). Inhibition curves are fitted from means of 3 separate experiments (the standard deviation never exceeding 10% of the mean). Inset: inhibition of HLE-mediated pro MMP-3 activation by OL-GAL derivatives. lane 1: pro MMP-3 (30 nM), lane 2: APMA activated pro MMP-3 (30 nM), lane 3: pro MMP-3 (30 nM) has been activated by 80 nM HLE, lane 4: HLE (80 nM) has been preincubated with 10 μ M OL-GAL (CONHOH) before adding pro MMP-3 (30 nM), lane 5: HLE (80 nM) has been preincubated with 10 μ M OL-GAL (COOH) before adding pro MMP-3 (30 nM).

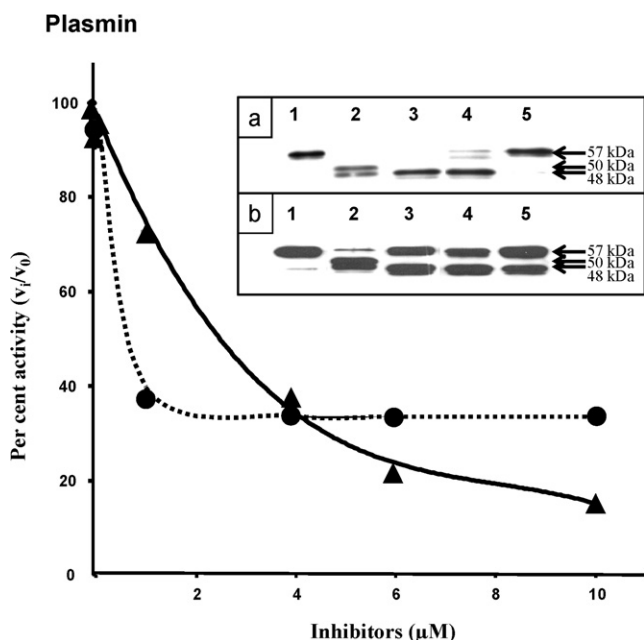


Fig. 6. Influence of oleoyl galardin derivatives on Plasmin amidolytic activity. abscissa: OL-GAL (CONHOH): ▲-▲; OL-GAL (COOH): ●-●; concentration (μM); ordinates: per cent activity (v_i/v_0). Inhibition curves are fitted from means of 3 separate experiments (the standard deviation never exceeding 10% of the mean). Inhibition of Plasmin-mediated proMMP-3 activation by OL-GAL derivatives.

Inset a: OL-GAL (CONHOH).

lane 1: pro MMP-3 (30 nM), lane 2: pro MMP-3 (30 nM) activated by APMA, lane 3: pro MMP-3 (30 nM) activated by plasmin (65 nM), lane 4: plasmin (65 nM) has been preincubated for 15 min with 1 μM OL-GAL (CONHOH) before adding pro MMP-3 (30 nM), lane 5: same as lane 4, except that OL-GAL (CONHOH) concentration was 10 μM.

Inset b: OL-GAL (COOH).

lane 1: pro MMP-3 (30 nM), lane 2: pro MMP-3 (30 nM) activated by APMA, lane 3: pro MMP-3 (30 nM) activated by plasmin (65 nM), lane 4: plasmin (65 nM) has been preincubated for 15 min with 1 μM OL-GAL (COOH) before adding pro MMP-3 (30 nM), lane 5: same as lane 4, except that OL-GAL (COOH) concentration was 10 μM.

collagens [39,40]. Interactions of human plasmin to natural substrates are directed by its kringle domains [18,28]; we previously evidenced that oleic acid bound avidly to plasmin kringle 5 ($K_D = 5.9 \times 10^{-8}$ M as determined by SPR analysis), further interfering with plasmin-mediated prostromelysin-1 activation [18]. Molecular docking simulations revealed that oleic acid can avidly bind to a groove comprising residues that can be part of kringles' canonical LBS [41].

Similarly as kringle 5, the Fn(II) domain of gelatinase A, i.e. MMP-2, contains two antiparallel beta sheets, a central $3_{(10)}$ -helix and similar orientation of the two proximal Cys–Cys bonds [42]. In keeping, oleic acid can interact with these Fn(II) domains, a property which contributes to the inhibition of the activity of gelatinase A. Preferential binding to Fn(II)₃ was here demonstrated with main involvement of Phe³⁵⁵ and Trp³⁷⁴. Of note, these residues within Fn(II)₃ domain were also implicated in the interaction of enzyme with gelatin [42] and type I collagen [43], thus possibly explaining the potent inhibitory capacity of oleic acid towards MMP-2-mediated gelatinolysis and collagenolysis *in vitro* and *ex vivo* [44]. However, it needs to be mentioned that, in solution, oleic acid was found to interact preferentially with Fn(II)₁ domain. Such discrepancy might rely from differences between the three-dimensional structure of pro MMP-2, resolved from X-ray crystallographic structure data, and the conformation of enzyme in solution. Indeed, a 32-residue sequence within the prodomain was reported to bind to Fn(II)₃; its loss, as occurring during enzyme activation, might induce main transconformation of Fn(II)₃ and

reorientation of these domains which tumble independently [27]. Although both K₅ and Fn(II) domains can bind to oleic acid, SPR analysis showed that fatty acid exhibited a 1000 fold higher affinity for K₅ as compared to Fn(II)₁. To that respect, molecular modeling indicated that oleic acid could also accommodate the S'₁ binding pocket of MMP-2, a finding consistent with the residual inhibitory capacity of fatty acid towards Fn(II)-deleted gelatinase A. However, unexpectedly, COOH group did not interact with Zn in MMP-2 active site, a finding consistent with data showing that replacement of COOH with hydroxamic acid had only minimal influence on the inhibitory potency of the compounds towards this enzyme as compared to differences (1000 fold) observed between other hydroxamate and carboxylate inhibitors of MMPs [45]. Of note, oleic acid proved to display potent inhibitory capacity towards MMP-13. Similarly to MMP-2, the long acid chain could position within S'₁ MMP-13 binding pocket but contrary to gelatinase, molecular docking indicates that carboxylic acid end group of fatty acid was able to chelate the Zn ion of MMP-13 active site.

Derivatization of several elastase inhibitors with oleic acid was previously envisaged at aims to obtain agents with improved potency, but also able to confer protection against matrix proteolysis in keeping with the ability of oleic acid to bind to fibronectin or elastin [14,46].

By analogy, we have introduced an oleoyl moiety at the P'₂ position of galardin, a broad spectrum MMP inhibitor. Generally, MMP S'₂ subsite consists of a shallow and solvent exposed pocket capable to accommodate several functionalities. However, with the exception of MMP-13, oleoyl-galardin(s), whatever in its COOH or CONHOH forms, were less potent as compared to parent galardin to inhibit MMPs. Molecular modeling, indicates that presence of the fatty acid can modify galardin skeleton binding mode; for instance, using MMP-2 as template, it was shown that the hydroxamic acid group in OL-GAL (CONHOH) does not bind Zn, but instead forms a salt bridge with Tyr¹¹⁰. That holds also true for MMP-13 when hydroxamic acid is strongly associated with Tyr¹⁷⁶, resulting in potent and selective inhibition of this MMP. Recent investigations pinpointed that potent and selective MMP-13 inhibitor could be obtained by non Zn-chelating compounds occupying S'₁ subsite [47,48].

Originally, one of our aim relied on the design of compounds able to bind simultaneously to S' subsites and Fn(II) domains of MMP-2. According to the literature, the distance between the Zn ion of the active site and the key tryptophan residue of the gelatin binding site was estimated to be 32 Å, but (PPG)₁₂-NHOH derivative that could cover such distance was found to exhibit low MMP-2 inhibitory capacity [49]. Molecular modeling studies using a hypothetical inhibitor from galardin allowed us to demonstrate that C19 type alkyl groups would be needed to reach the rims of the Fn(II)₃ domains, i.e. (not shown) Arg³⁶⁸ and Trp³⁸⁷. Whether we would like to reproduce entirely the binding mode of oleic acid, a C32 type alkyl group should be added to P'₂ subsite of galardin (not shown). Obviously, the size and the great flexibility of such an inhibitor could be problematic.

Nevertheless, these OL-GAL derivatives, could inhibit elastase activity and also could interfere with HLE and also with plasmin-mediated pro MMP-3 activation thus acting at several levels in the proteolytic cascades during chronic inflammation. Besides, simultaneous inhibition of plasmin, elastase, stromelysin-1 and particularly collagenase-3 make these compounds as putative therapeutic agents in chronic inflammatory disorders and diseases as rheumatoid arthritis and cancer [49–54].

Acknowledgements

This research was supported in part by a Grant-in-Aid «Contrat de Plan Etat-Région» 2007–2013 and FEDER funds.

AJPA and GM thank the Comité de l'Aisne contre le Cancer for grant funding.

Our acknowledgements are due to C Guillaume and S Noizet for technical support.

Appendix A. Supplementary data

Supplementary data associated with this article can be found, in the online version, at doi:10.1016/j.bcp.2010.12.001.

References

- [1] Eming SA, Krieg T, Davidson JM. Inflammation in wound repair: molecular and cellular mechanisms. *J Invest Dermatol* 2007;127:514–25.
- [2] Toriseva M, Kähri VM. Proteinases in cutaneous wound healing. *Cell Mol Life Sci* 2009;66:203–24.
- [3] Trengrove NJ, Stacey MC, MacAuley S, Bennett N, Gibson AJ, Burslem F, et al. Analysis of the acute and chronic wound environments: the role of proteases and their inhibitors. *Wound Rep Reg* 1999;7(6):442–52.
- [4] Gill SE, Parks WC. Metalloproteinases and their inhibitors: regulators of wound healing. *Int J Biochem Cell Biol* 2008;40:1334–47.
- [5] Barrick B, Campbell EJ, Owen CA. Leukocyte proteinases in wound healing: roles in physiologic and pathologic processes. *Wound Rep Reg* 1999;7:410–22.
- [6] Saarialho-Kere UK. Patterns of MMPs and TIMP expression in chronic wounds. *Arch Dermatol Res* 1998;290(Suppl.):547–54.
- [7] Nagase H, Visse R, Murphy G. Structure and function of matrix metalloproteinases and TIMPs. *Cardiovasc Res* 2006;69:562–73.
- [8] Page-McCaw A, Ewald AJ, Werb Z. Matrix metalloproteinases and the regulation of tissue remodelling. *Nat Rev Mol Cell Biol* 2007;8:221–33.
- [9] Shapiro SD, Goldstein NM, Houghton AM, Kobayashi DK, Kelley D, Belaaouaj A. Neutrophil elastase contributes to cigarette smoke-induced emphysema in mice. *Am J Pathol* 2003;163(6):2329–35.
- [10] Park YS, Jang HJ, Lee KH, Hahn TR, Paik YS. Prolyl endopeptidase inhibitory activity of unsaturated fatty acids. *J Agric Food Chem* 2006;54(4):1238–42.
- [11] Kido H, Fukusen N, Katunama N. Inhibition of chymase activity by long chain fatty acids. *Arch Biochem Biophys* 1984;230(2):610–4.
- [12] Hamel FG. Preliminary report: inhibition of cellular protease activity by free fatty acids. *Metabolism* 2009;58(8):1047–9.
- [13] Wang D, Girard TJ, Kasten TP, LaChance RM, Miller-Wideman MA, Durley RC. Inhibitory activity of unsaturated fatty acids and anacardic acids toward soluble tissue factor-factor VIIa complex. *J Nat Prod* 1998;61(11):1352–5.
- [14] Hornebeck W, Moczar E, Szececi J, Robert L. Fatty acid peptide derivatives as model compounds to protect elastin against degradation by elastases. *Biochem Pharmacol* 1985;34(18):3315–21.
- [15] Tyagi SC, Simon SR. Inhibitors directed to binding domains in neutrophil elastase. *Biochemistry* 1990;29:9970–7.
- [16] Shock A, Baum H, Kapasi MF, Bull FM, Quinn PJ. The susceptibility of elastin-fatty acid complexes to elastolytic enzymes. *Matrix* 1990;10(3):179–85.
- [17] Berton A, Rigot V, Huet E, Decarme M, Eeckhout Y, Patthy L, et al. Involvement of fibronectin type II repeats in the efficient inhibition of gelatinases A and B by long-chain unsaturated fatty acids. *J Biol Chem* 2001;276(23):20458–65.
- [18] Huet E, Cauchard JH, Berton A, Robinet A, Decarme M, Hornebeck W, et al. Inhibition of plasmin-mediated prostromelysin-1 activation by interaction of long chain unsaturated fatty acids with kringle 5. *Biochem Pharmacol* 2004;67(4):643–54. Erratum in: *ibid* 2004;67(5):1011.
- [19] Kerneur C, Hornebeck W, Robert L, Moczar E. Inhibition of human leukocyte elastase by fatty acyl-benzisothiazolinone, 1,1-dioxide conjugates (fatty acyl-saccharins). *Biochem Pharmacol* 1993;45(9):1889–95.
- [20] Baici A, Diczhazi C, Neszmelyi A, Moczar E, Hornebeck W. Inhibition of the human leukocyte endopeptidases elastase and cathepsin G and of porcine pancreatic elastase by N-oleoyl derivatives of heparin. *Biochem Pharmacol* 1993;46(9):1545–9.
- [21] Kunishima M, Kawachi C, Morita J, Terao K, Iwasaki F, Tani S. 4-(4,6-dimethoxy-1,3,5-triazin-2-yl)-4-methyl-morpholinium chloride: an efficient condensing agent leading to the formation of amides and esters. *Tetrahedron* 1999;55:13159–70.
- [22] Lewis N, McKillop A, Taylor R, Watson R. A simple and efficient procedure for the preparation of chiral 2-oxazolidinones from α -amino acids. *Synth Commun* 1995;25:561–8.
- [23] Morris GM, Goodsell DS, Halliday RS, Huey R, Hart WE, Belew RK, et al. Automated docking using a Lamarckian genetic algorithm and an empirical binding free energy function. *J Comput Chem* 1998;19:1639–62.
- [24] Huey R, Morris GM, Olson AJ, Goodsell DS. A semiempirical free energy force field with charge-based desolvation. *J Comput Chem* 2007;28(6):1145–52.
- [25] Frisch MJ, Trucks GW, Schlegel HB, Scuseria GE, Robb MA, Cheeseman JR, et al. Gaussian 03, Revision B.05. Wallingford, CT: Gaussian, Inc.; 2004.
- [26] Bode W, Wei AZ, Huber R, Meyer E, Travis J, Neumann S. X-ray crystal structure of the complex of human leukocyte elastase (PMN elastase) and the third domain of the turkey ovomucoid inhibitor. *EMBO J* 1986;5(10):2453–8.
- [27] Morgunova E, Tuuttila A, Bergmann U, Isupov M, Lindqvist Y, Schneider G, et al. Structure of human pro-matrix metalloproteinase-2: activation mechanism revealed. *Science* 1999;284(5420):1667–70.
- [28] Battistel MD, Grishaev A, An SS, Castellino FJ, Llinás M. Solution structure and functional characterization of human plasminogen kringle 5. *Biochemistry* 2009;48(43):10208–19.
- [29] Blagg JA, Noe MC, Wolf-Gouveia LA, Reiter LA, Laird ER, Chang SP, et al. Potent pyrimidinetrione-based inhibitors of MMP-13 with enhanced selectivity over MMP-14. *Bioorg Med Chem Lett* 2005;15(7):1807–10.
- [30] Li H, Robertson AD, Jensen JH. Very fast empirical prediction and rationalization of protein pKa values. *Proteins* 2005;61(4):704–21.
- [31] Bas DC, Rogers DM, Jensen JH. Very fast prediction and rationalization of pKa values for protein-ligand complexes. *Proteins* 2008;73(3):765–83.
- [32] Cook L, Termai B. Similar binding sites for unsaturated fatty acids and alkyl 2-pyrone inhibitors of human sputum elastase. *Biol Chem Hoppe Seyler* 1988;369(7):627–31.
- [33] Moroy G, Denhez C, El Mourabit H, Toribio A, Dassonville A, Decarme M, et al. Simultaneous presence of unsaturation and long alkyl chain at P₁ of Ilomastat confers selectivity for gelatinase A (MMP-2) over gelatinase B (MMP-9) inhibition as shown by molecular modelling studies. *Bioorg Med Chem* 2007;15(14):4753–66.
- [34] Ledour G, Moroy G, Rouffet M, Bourguet E, Guillaume D, Decarme M, et al. Introduction of the 4-(4-bromophenyl)benzenesulfonyl group to hydrazide analogs of Ilomastat leads to potent gelatinase B (MMP-9) inhibitors with improved selectivity. *Bioorg Med Chem* 2008;16(18):8745–59.
- [35] Emonard H, Marcq V, Mirand C, Hornebeck W. Inhibition of gelatinase A by oleic acid. *Ann N Y Acad Sci* 1999;878:647–9.
- [36] Levy DE, Lapiere F, Liang W, Ye W, Lange CW, Li X, et al. Matrix metalloproteinase inhibitors: a structure-activity study. *J Med Chem* 1998;41:199–223.
- [37] Nagase H. Activation mechanisms of matrix metalloproteinases. *Biol Chem* 1997;378:151–60.
- [38] Nagase H, Enghild JJ, Susuki K, Salvesen G. Stepwise activation mechanisms of the precursor of matrix metalloproteinase 3 (stromelysin) by proteinases and (4-aminophenyl) mercuric acetate. *Biochemistry* 1990;29(324):5783–9.
- [39] Lauer-Fields JL, Whitehead JK, Li S, Hammer RP, Brew K, Fields GB. Selective modulation of matrix metalloproteinase 9 (MMP-9) functions via exosite inhibition. *J Biol Chem* 2008;283(29):20087–95.
- [40] Xu X, Chen Z, Wang Y, Bonewald L, Steffensen B. Inhibition of MMP-2 gelatinolysis by targeting exodomain-substrate interactions. *Biochem J* 2007;406:147–55.
- [41] Frank PS, Douglas JT, Locher M, Llinas M, Schaller J. Structural/functional characterization of the alpha 2-plasmin inhibitor C-terminal peptide. *Biochemistry* 2003;42(4):1078–85.
- [42] Trexler M, Briknarova K, Gehrmann M, Llinas M, Patthy L. Peptide ligands for the fibronectin type II modules of matrix metalloproteinase 2 (MMP-2). *J Biol Chem* 2003;278(14):12241–6.
- [43] Xu X, Mikhailova M, Ilangovan U, Chen Z, Yu A, Pal S, et al. Nuclear magnetic resonance mapping and functional confirmation of the collagen binding sites of matrix metalloproteinase-2. *Biochemistry* 2009;48:5822–31.
- [44] Berton A, Godeau G, Emonard H, Baba K, Bellon P, Hornebeck W, et al. Analysis of the ex vivo specificity of human gelatinases A and B towards skin collagen and elastic fibers by computerized morphometry. *Matrix Biol* 2000;19(2):139–48.
- [45] Grobely D, Poncz L, Galardy RE. Inhibition of human skin fibroblast collagenase, thermolysin, and *Pseudomonas aeruginosa* elastase by peptide hydroxamic acids. *Biochemistry* 1992;31(31):7152–4.
- [46] Stanislawski L, Hornebeck W. Effect of sodium oleate on the hydrolysis of human plasma fibronectin by proteinases. *Biochem Int* 1988;16(4):661–70.
- [47] Heim-Riether A, Taylor SJ, Liang S, Gao DA, Xiong Z, August EM, et al. Improving potency and selectivity of a new class of non-Zn-chelating MMP-13 inhibitors. *Bioorg Med Chem Lett* 2009;19:5321–4.
- [48] Gooljarsingh LT, Lakdawala A, Coppo F, Luo L, Fields GB, Tummino PJ, et al. Characterization of an exosite binding inhibitor of matrix metalloproteinases 13. *Prot Sci* 2008;17:66–71.
- [49] Jani M, Tordai H, Trexler M, Banyai L, Patthy L. Hydroxamate-based peptide inhibitors of matrix metalloproteinase 2. *Biochimie* 2005;87:385–92.
- [50] Momohara S, Kashiwasaki S, Inoue K, Saito S, Nakagawa T. Elastase from polymorphonuclear leukocyte in articular cartilage and synovial fluids of patients with rheumatoid arthritis. *Clin Rheumatol* 1997;16(2):133–40.
- [51] Matsuno H, Yudoh K, Watanaba Y, Nakazawa F, Aono H, Kimura T. Stromelysin-1 (MMP-3) in synovial fluid of patients with rheumatoid arthritis has potential to cleave membranes bound Fas ligand. *J Rheumatol* 2001;28(1):22–8.
- [52] Takaishi H, Kimura T, Dlai S, Okada Y, D'Armiento J. Joint diseases and matrix metalloproteinases: a role for MMP-13. *Curr Pharm Biotechnol* 2008;9(1):47–54.
- [53] Cox SW, Eley BM, Kiili M, Asikainen A, Tervahartiala T, Sorsa T. Collagen degradation by interleukine 1 β -stimulated gingival fibroblasts is accompanied by release and activation of multiple matrix metalloproteinases and cysteine proteinases. *Oral Dis* 2006;12:34–40.
- [54] Bourguet E, Sapi J, Emonard H, Hornebeck W. Control of melanoma invasiveness by anticollagenolytic agents: a reappraisal of an old concept. *Anticancer Agents Med Chem* 2009;9(5):576–9.